



The effect of lithium loadings on anode to the voltage drop during charge and discharge of Li-ion capacitors



W.J. Cao ^{a, b}, M. Greenleaf ^{a, b}, Y.X. Li ^d, D. Adams ^{a, b}, M. Hagen ^{a, b}, T. Doung ^e,
J.P. Zheng ^{a, b, c, *}

^a Department of Electrical and Computer Engineering, Florida A&M University and Florida State University, Florida State University, Tallahassee, FL, 32310, USA

^b Aero-Propulsion, Mechatronics and Energy (AME) Center, Florida State University, Tallahassee, FL, 32310, USA

^c Center for Advanced Power Systems (CAPS), Florida State University, Tallahassee, FL, 32310, USA

^d FMC Lithium Division, Bessemer City, NC, 28016, USA

^e Office of Vehicle Technologies, U.S. Department of Energy, Annandale, VA, 22003, USA

H I G H L I G H T S

- Investigated the voltage drop from Li-ion capacitors during charge and discharge.
- Demonstrated the importance of loadings of the stabilized lithium metal powders in Li-ion capacitors.
- Discussed mechanisms for causing the voltage drop of Li-ion capacitors.

A R T I C L E I N F O

Article history:

Received 10 November 2014

Received in revised form

3 January 2015

Accepted 14 January 2015

Available online 16 January 2015

Keywords:

Li-ion capacitor

Hard carbon

IR-drop

SLMP loadings

Electrochemical impedance spectroscopy

(EIS)

Equivalent circuit modeling

A B S T R A C T

The IR voltage drop from the anode and cathode of Li-ion capacitors during charge and discharge was studied. Li-ion capacitors were made with activated carbon cathode and hard carbon anode with different loadings of stabilized lithium metal powder (SLMP). It was found that the LICs with high SLMP loadings showed smaller voltage drop than LICs with low SLMP loadings. It was also found that at low SLMP loadings, the IR voltage drops at high cell voltages were smaller than that at low cell voltages; while at high SLMP loadings, small IR voltage drops were obtained for both low and high cell voltages. The electrochemical impedance spectroscopy confirmed that voltage drops are directly related to the internal resistances of Li-ion capacitors.

© 2015 Elsevier B.V. All rights reserved.

1. Introduction

Pursuing more efficient energy storage devices which can provide high energy density, good power performance and long cycle life is always a popular research topic all over the world. The conventional electrochemical double-layer capacitors (EDLCs), which contain two symmetrical activated carbon electrodes with high surface area and porous structure, have the characteristics of high

power and long cycle life; However, the energy density of the EDLCs is less than 10% of that of a lithium (Li)-ion batteries (LIBs), which restricts its application in many fields including hybrid electric vehicles (HEVs), electric vehicles (EVs) and other large-scale energy storage systems. Therefore, in recent years considerable research has been focused on the development of higher energy density supercapacitors. Among all the energy storage systems that have been investigated and developed in the last years, Li-ion Capacitors (LICs) have emerged to be one of the most promising because LICs can achieve higher energy density than conventional EDLCs, and better power performance than LIBs as well being capable of long cycle life. LICs contain a pre-lithiated LIB anode electrode and an

* Corresponding author. FSU AME building, 2003 Levy Ave, Tallahassee, FL, 32304, USA.

E-mail address: zheng@eng.fsu.edu (J.P. Zheng).

EDLC cathode electrode [1–3].

Extensive research has been done to optimize the electrochemical performance of the LICs [4–21]. Recently, Puthusseri et al. [22] improved the energy density of LICs using polymer-derived porous carbons as cathode; Ren et al. [23] utilized pre-lithiated graphene nanosheets as negative electrode materials to achieve high power and energy density LICs; Schroeder et al. [24] compared the soft carbon and graphite anode material in the electrochemical performance in LICs, and found that soft carbon represented a promising alternative to graphite especially in the high rates applications. In the LICs energy storage system, anode pre-lithiation is a key process for assembling the LICs. Fuji Co. [6] proposed that a third electrode of Li metal can be used for pre-lithiation of the graphite electrodes as shown in Fig. 1. The first company to utilize a third electrode of Li metal to pre-lithiate the anode and produce LICs was JM Energy and the energy density of their LICs reached approximately 10 Wh/kg with a very stable cycle life.

Stabilized Li metal powder (SLMP[®]) is a pioneering and revolutionary material and technology developed by FMC that is able to provide electrochemically energy carrier as rechargeable Li atom for all types of Li based energy devices. SLMP is comprised of spherical particles with controlled particle size and surface area. SLMP is made by agitating a mixture of molten Li metal in a hydrocarbon oil at dispersion speeds [25,26]. The thickness and chemistry of the protective coating layer can be tailored and engineered based on user preference. SLMP can offer a capacity as high as 3600 mAh/g [27] and still can be safely introduced to the energy storage devices in a dry room atmosphere. Extensive studies have been done using SLMP in Li-ion battery energy storage systems [27–30]. Previously, we have reported a LIC with activated carbon (AC) cathode and hard carbon (HC)/SLMP anode electrodes with high energy density, high power density and long cycle life [31–34,47,48]. Instead of using a third Li foil electrode to pre-

lithiate the anode, our group was the first to propose a pre-lithiation process by method of pressing SLMP on the surface of hard carbon anode electrodes in the LICs energy storage systems as displayed in Fig. 2. After the SLMP was applied onto the surface of the hard carbon anode electrodes, Li from the SLMP intercalated into the hard carbon when the electrolyte was filled into the cell. SLMP provides electrochemically active Li source as the energy carrier for capacitor. This high energy density concept of the LIC with such a novel structure as a conventional two-electrode rather than three-electrode cell has already been demonstrated in the laboratory using both coin cells and pouch cells [31–34,47,48]. As such, the usage of expensive copper mesh used to attach Li metal foil in three-electrode configuration as developed by Fuji Co. [6] is avoided.

Compared to the EDLCs having applied aqueous electrolytes with high conductivity, the LICs using nonaqueous electrolytes have serious problems with high power performance because of the overpotential on the high rate charge–discharge process. Usually, an Ohmic drop due to the electronic or ionic current flow, and a decrease in the voltage that is used for driving the reactions and the concentration gradients in a test cell [20] result in the IR drop in LICs. Despite numerous papers that have been published on the LICs, very few reports have discussed the effects of anode SLMP loadings on the IR drop of LICs in detail.

A useful tool in evaluating the effectiveness of the SLMP loading is electrochemical impedance spectroscopy (EIS), a process by

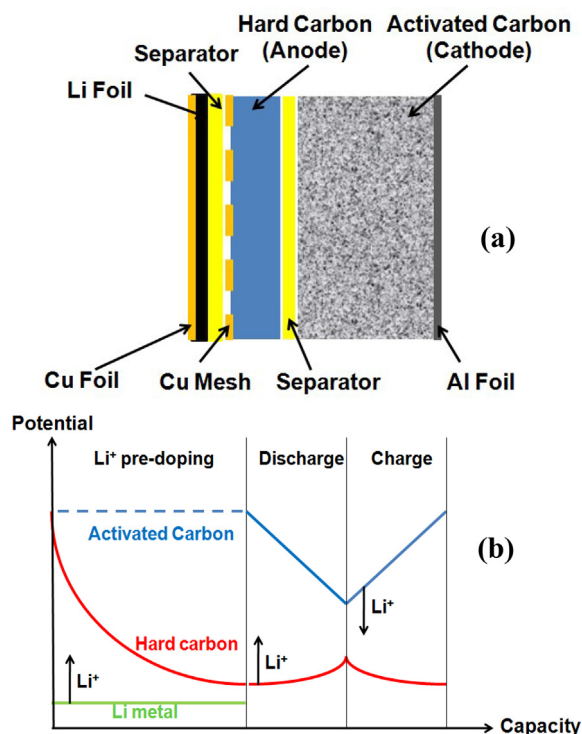


Fig. 1. (a) A schematic diagram of a three-electrodes (Li foil as the third electrode) Li-ion capacitor configuration and (b) the charge transfer between three electrodes during initial charge and discharge cycling.

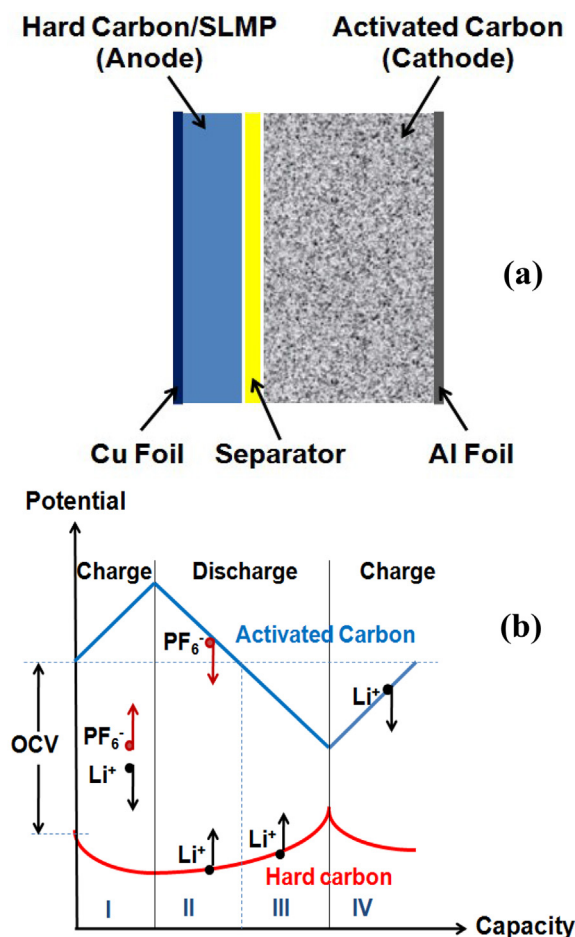


Fig. 2. (a) A schematic diagram of the AC/HC-SLMP novel two-electrodes Li-ion capacitor configuration and (b) schematic ion transfer in the Li-ion capacitor when the cell voltage greater (I and II) and lower (III and IV) than OCV.

which frequency-dependent data may be obtained in a non-destructive manner. Commonly, the EIS data may be evaluated using an equivalent circuit model which may be used to fit the data and recover electrochemical reaction-specific information about the cell, including—but not limited to—charge transfer kinetics, diffusion, mass transfer, and solution resistance [42].

Hence, in this paper, we wish to report the detailed comparative study of IR drops for the LICs with various anode SLMP loadings. The comparison of the EIS of all the LIC cells and a developed equivalent circuit model detailing the SLMP loading effect on the impedance spectra is also reported in this paper.

2. Experimental

Commercial materials were used as both the positive and negative electrodes. The positive electrode was prepared by coating a slurry mixture of activated carbon and the polytetrafluoroethylene (PTFE) as the binder by the mass ratio of 94:6 on a 20 μm -thick Al foil substrate. The slurry mixture of the negative electrode (NE) was composed of hard carbon and PTFE as a binder by the mass ratio of 96:4. After the slurry was prepared, it was coated onto a Cu foil substrate that had a thickness of 10 μm . Then the electrodes were dried at 120 $^{\circ}\text{C}$ for 12 h in an oven with constant flowing air. After the electrodes were dried, the AC and HC electrode sheets were compressed by heated-rolling mill to compress them to the desired thickness of 100 μm for AC and 85 μm for HC. All the electrode sheets were kept in a dry room (Dew Point -30°C) and punched out into 2 cm^2 (active area) round disks. All the cut electrodes were additionally dried at 120 $^{\circ}\text{C}$ overnight in a vacuum oven. After drying, the HC anode electrodes were surface treated with various amounts of SLMP followed by pressing with a rolling mill in the dry room before being assembled into Li-ion capacitor test cells. SLMP is Li metal powder with a passivation layer on its surface with an average particle size of ~ 40 μm . The electrolyte was 1 M LiPF_6 in ethylene carbonate (EC): dimethyl carbonate (DMC) at a ratio of 1:1 by weight and the separator was a 50 μm -thick glass fiber.

Four three-electrode LIC test cells (ECC-Ref, EL-CELL Germany) with different SLMP loadings on anode were assembled in an Argon-filled glove box (<1 ppm oxygen and moisture) and discharged and charged from 2.0 to 4.0 V under a constant current of 10 mA for 3 cycles, while the potentials of anode and cathode vs. Li/Li^+ reference electrode were monitored in order to determine the

potential for both anode and cathode. The EIS of all the test cells at the voltages of 4 and 2 V were recorded and the resulted spectrums were fitted by an equivalent circuit model in Scribner Associates' ZView program; An Arbin BT-2000 Battery Testing Unit was used for performance test and the electrochemical impedance spectrum (EIS) of LIC cells was recorded in the frequency range of 0.01– 10^6 Hz with an amplitude of 10 mV using Gamry Instruments Reference 3000 Potentiostat/Galvanostat/ZRA.

3. Results and discussion

Four three-electrode LIC test cells with no, low, medium and high SLMP loadings on anode were assembled and tested. The weight of the cathode AC electrodes was about 11.3 mg, the weight of the anode HC electrodes was about 20.6 mg, the SLMP loadings were 0, 1.4, 2.06, and 2.6 mg which will be referred as no, low, medium, and high loading, respectively. It should be pointed out that the capacity of the anode is much higher than that of the cathode. It is due to an overall consideration of internal resistance of the anode and the cycle life of the LIC. The potential profile vs. capacity of the HC was showed in previous paper [33] and is similar shape to Fig. 3. The useable capacity of the HC will be limited in the potential range around 0.2–0.5 V vs. Li/Li^+ , because at potential above 0.5 V vs. Li/Li^+ , the internal resistance of the HC is too high to limit the maximum power of the LIC; and at potential below 0.2 V vs. Li/Li^+ , the solid electrolyte interface (SEI) layer growth rate is too high to limit the cycle life of the LIC. The open-circuit potentials of anodes were measured as shown in Fig. 3. It can be seen that the potential of anode reduced with increasing the loading of SLMP due to the Li intercalation into the HC. Fig. 4 shows the galvanostatic charge–discharge profiles measured from the three-electrode configuration for the first two cycles of the LICs with various SLMP loadings on anode. The anode and cathode potentials were recorded vs. a Li/Li^+ reference electrode. The cell voltage was calculated from the potential difference between cathode and anode potentials as shown in Fig. 1. Table 1 summarized anode and cathode potentials, IR drops due to constant current charge and discharge from the anode and cathode at cell voltages of 2 and 4 V for four cells with different SLMP loadings. The reason for measurements to be carried at cell voltages of 2 and 4 V is because they represent the minimum and maximum cell voltages, respectively, for LICs. It can be seen that the potentials of both anode and cathode reduced with increasing the SLMP loading. Because more SLMP loading was applied to the anode, more Li intercalated into anode occurred which resulted a lower potential [33]. From Table 1, it can also be seen that (1) the IR drop from anode was greater than that from cathode, particularly, large values of IR drops were obtained from anodes with no and low SLMP loadings. Overall IR drops from cells were 0.25–0.27 V for medium–high SLMP loadings, 0.59 V for low SLMP loading, and as high as 1 V for no SLMP loading; and (2) for no and low SLMP loading on the anode, the IR drop of at the cell voltage of 2 V was greater than that at 4 V. Therefore, the experimental results clearly showed that the SLMP loading to the anode in LICs not only determined the potential of the anode and the cyclability [33], but also determined the IR drop as well as maximum power of the LIC cells.

Fig. 5 displays the EIS measured from 3-electrode LIC cells with different SLMP loadings at cell voltages of 2.0 and 4.0 V. It can be seen that for the LIC cell with no SLMP loading, the resistance at 2 V is much greater than that at 4 V. The resistances at the frequency of 0.01 Hz are about 650 and 17 Ω at 2 and 4 V, respectively; for the LIC cell with low SLMP loading, the resistance at 2 V is also greater than that at 4 V; however, for the LIC cells with medium and high SLMP loadings, the EISs at 2 and 4 V are very similar. The resistances at

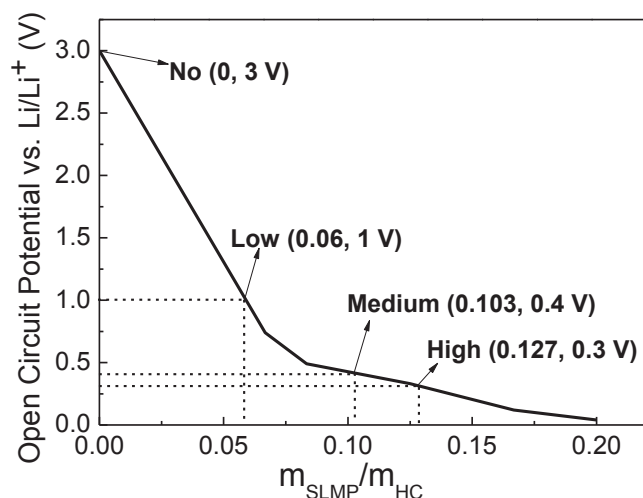


Fig. 3. The open-circuit potentials of anodes as a function of the SLMP loadings.

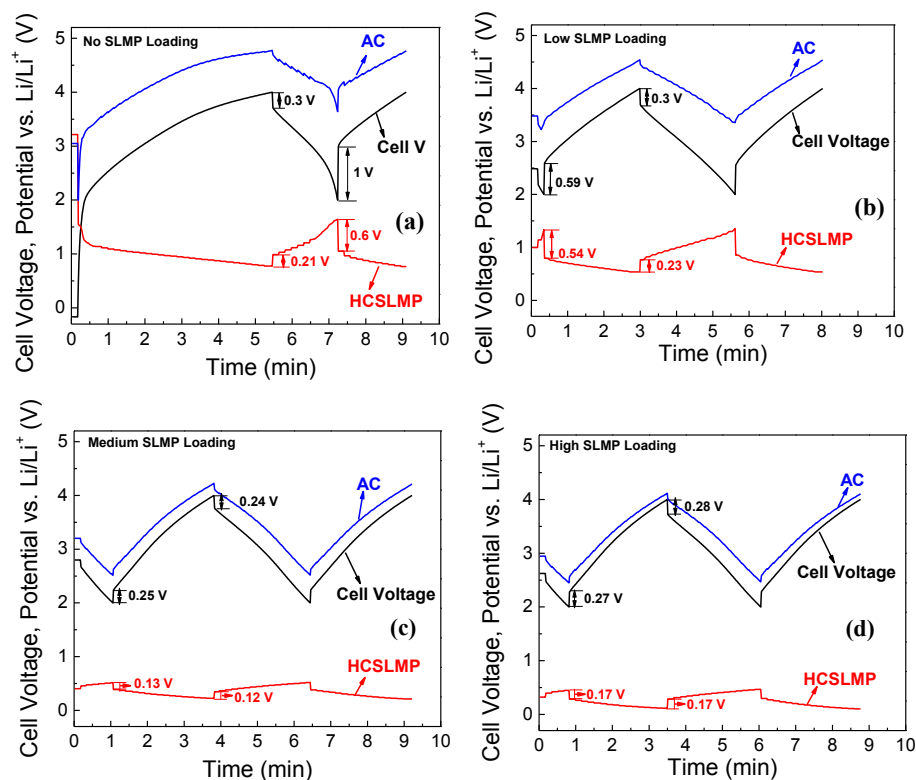


Fig. 4. Galvanostatic charge–discharge profiles measured from a 3-electrode configuration for the first cycle of Li-ion capacitor with (a) no, (b) low, (c) medium, and (d) high SLMP loadings on anode.

Table 1

Summary of the cell voltage, cathode and anode potential, and their IR drop under the different SLMP loadings on anode.

SLMP loading	Cell voltage (V)	Cathode potential vs. Li/Li^+ (V)	Anode potential vs. Li/Li^+ (V)	Cathode IR drop (V)	Anode IR drop (V)	Cell IR drop (V)
No	4	4.77	0.77	0.09	0.21	0.3
Low	4	4.54	0.54	0.07	0.23	0.3
Medium	4	4.22	0.22	0.12	0.12	0.24
High	4	4.11	0.11	0.11	0.17	0.28
No	2	3.64	1.64	0.4	0.6	1
Low	2	3.33	1.33	0.05	0.54	0.59
Medium	2	2.52	0.52	0.12	0.13	0.25
High	2	2.45	0.45	0.1	0.17	0.27

0.01 Hz are about 15 Ω at cell voltages of 2 and 4 V. The observation of the resistance change is consistent with the previous IR drop results.

An equivalent circuit model was used to fit EIS curves obtained from 3-electrode LIC cells with low and high SLMP loadings. Fig. 6(a) shows the equivalent circuit model which can be used to describe various physical and electrochemical processes inside LICs. In the model: L represents the wire inductance of leads and wires; R_s represents the ohmic resistances including contacts, separator paper, and electrolyte solution [35,36]; R_{SEI} and C_{SEI} represent the solid electrolyte interface (SEI) layer [37,38] which, in this case, is on the surface of the Li-metal powder on the carbon anode and commonly found on carbon anodes; R_{ct} is the charge transfer resistance, a non-ohmic resistance related to the exchange current density, while C_{dl} is the double layer of charge formed at the electrolyte/electrode boundary [39,40]. Lastly Z_{W0} represents the finite state Warburg element which describes diffusion of ions with a reflecting boundary [37,41–44].

By applying this phenomenological model to the EIS data collected and represented in Fig. 5, a frequency-domain fitting was carried out to determine the qualitative effects SLMP loading had on the electrochemical impedance response of the prepared 3-electrode LIC cells. This qualitative fitting data was then used to observe the effect SLMP loading had on various electrochemical processes represented by their matching circuit element analogs. It should be noted that the fitting of the EIS data was not intended to provide a high-accuracy fitting as all of the electrochemical mechanisms inside the 3-electrode LIC cells were not modeled. It was, instead, the purpose of this fitting to broadly observe trends in more visible processes (i.e. diffusion, charge transfer kinetics, ohmic contact resistance) which provided useful information regarding the effect SLMP loading had on the cells.

Fig. 6(b) provides an example cell fitting using the equivalent circuit in Fig. 6(a) to fit the EIS data of the low SLMP loaded full-cell at 2.0 V. By implementing this equivalent circuit model to the EIS data collected, the evolution of circuit parameters with varying voltages and SLMP loading states may be generally discussed. From Table 2, it can be seen that increasing SLMP loading significantly reduces the Warburg resistance by a factor of 4, reduces the charge transfer resistance by a factor of 7, and increases the Warburg capacitance by 28% at 2.0 V. In the case of the Warburg resistance, the activated carbon electrode reduces to a voltage below 3.0 V vs. Li/Li^+ for high SLMP loading allowing Li cations to diffuse into the activated carbon matrix. This does not occur in the Low SLMP loading case in which only the larger PF_6^- anions diffuse into the activated carbon matrix. The smaller radii of Li^+ when compared to PF_6^- likely yields a larger diffusion coefficient for the high SLMP loaded cell at 2.0 V which, in turn, yields a lower Warburg resistance value.

By analysis of experimental results from galvanostatic

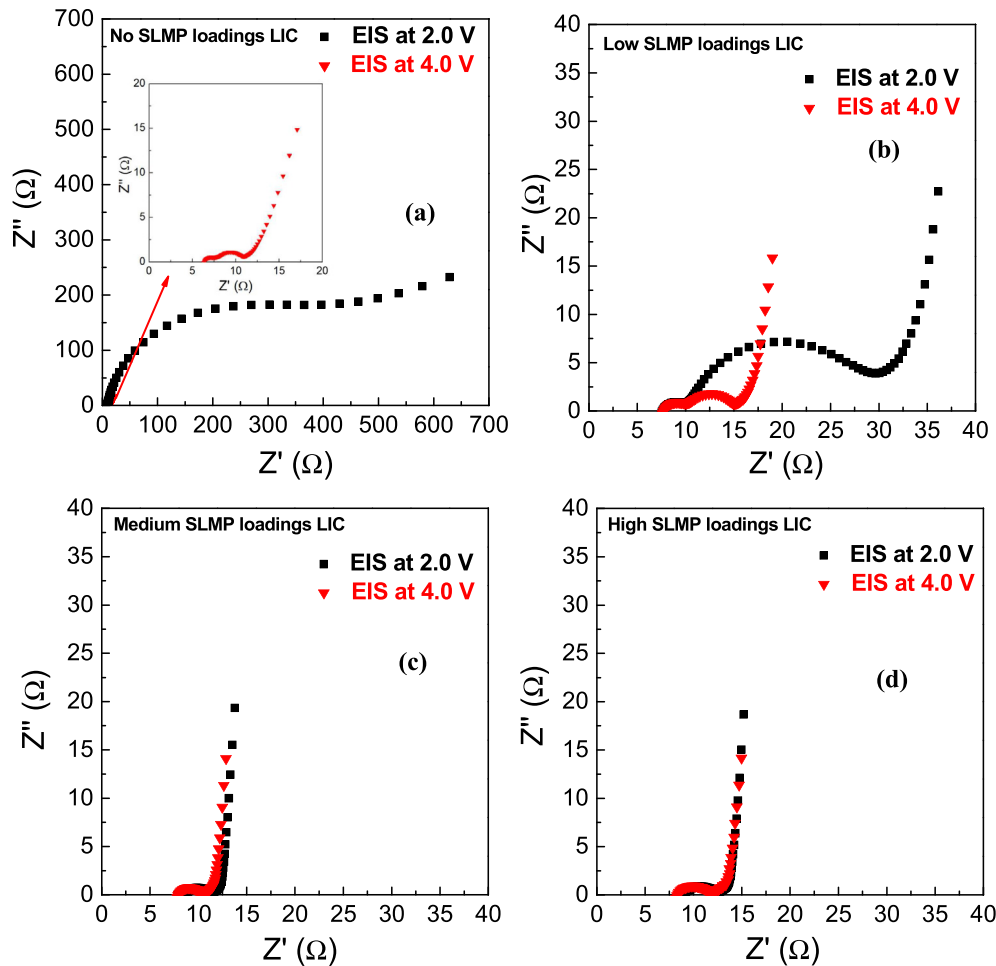


Fig. 5. The EIS for Li-ion capacitor test cell with (a) no, (b) low, (c) medium, and (d) high SLMP loadings on anode at cell voltages of 2.0 and 4.0 V.

charge–discharge profiles and EIS curves at different voltages for cells made with various SLMP loadings, it can be concluded that (1) the IR-drop was dominated by anode and (2) the IR-drop at anode increased with decreasing the potential of the anode. In other words, the overall IR-drop of a LIC was mainly determined by the potential of the anode, which meant that the resistance for the IR drop was influenced by the potential of the anode. And the potential of anode depended on how much SLMP intercalation into the HC anode electrodes. It is obvious that higher SLMP loadings lead to more Li intercalating into the HC electrodes. This conclusion is consistent with the observation of structure change in HC during the lithiation process by Nagao et al. [46]. They have studied the HC structure using x-ray and neutron scattering and concluded that the Li can be inserted into the periodically layered structure of HC and such lithiation can be divided into two regions—shallow and deep. In the shallow lithiation region the distance between layers didn't change, while the distance between layers increased with increasing the degree of the lithiation in the deep lithiation region. To understand the voltage drops of HC anodes at no or low loading of SLMP the HC was in shallow lithiation region. The distance of c–c layer was small and the resistance of Li intercalation was large; however, at medium and high loading of SLMP, the HC was in the deep lithiation region. The distance of c–c layers increased and the resistance of Li intercalation also decreased. Above all, it can be concluded that the different loadings of SLMP made the different degrees of the lithiation in the HC. At no to low loadings of SLPM, the anode

located at high potential range, the lithiation processes must overcome a c–c layers extension processes which appeared a high internal resistance; however, at mediate to high loadings of SLMP, which led to various distance of c–c layers and different potentials of the anode. These different c–c layer distances and potentials of the anode varied the resistances for the Li intercalation so that the total resistance and IR drop of the LICs will be influenced and varied. From our previous study [47], it has concluded that the loading of SLMP would directly affect the electrochemical performance of LICs including energy, power, and cycling, and optimal loadings of SLMP is 10.3–12.7% of HC at anode.

Lastly, it is also shown in Table 2 that the Warburg capacitances which represent the total capacitances stored in the diffusion channel of the activated carbon electrodes can be calculated by $C_{W0} = T_{W0}/R_{W0}$ and are in a range of 0.71–1.12 F, which is consistent with the measurement from dc charge and discharge as shown in Fig. 3. A comparison between calculated capacitance and directly measured capacitance was listed in Table 3. It can be seen that the capacitance increased 28% when SLMP loading was increased.

4. Conclusion

It was found that IR-drop during charge and discharge of a LIC is strongly dependent on the loading of the SLMP on the anode and the potential of the anode. When a sufficient amount of SLMP was applied to the anode, the IR-drop of the LIC reduced and was less

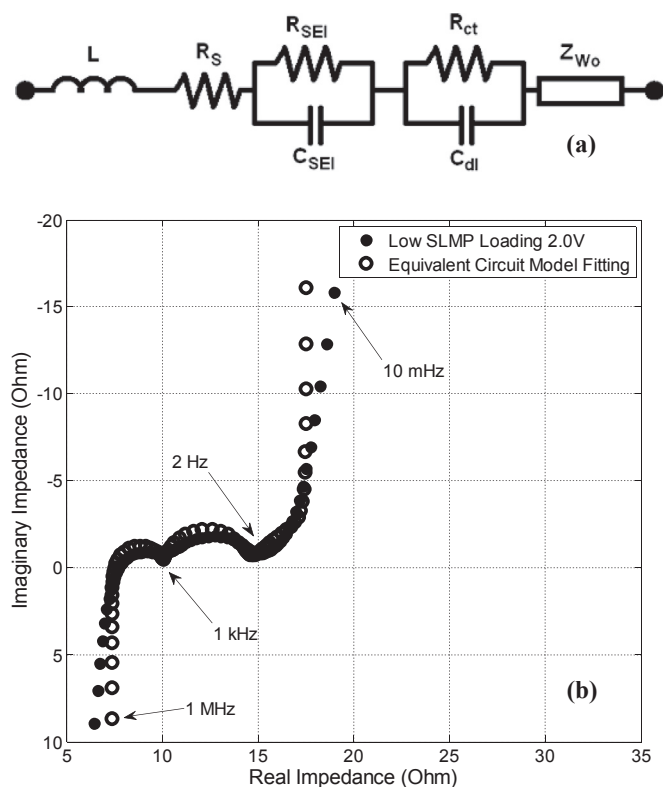


Fig. 6. (a) Equivalent circuit model representing the LIC full-cell in the frequency domain and (b) fitting of Nyquist plot using equivalent circuit model for low SLMP loaded cell.

Table 2
LIC full-cell equivalent circuit parameters.

U (V)	SLMP loading	L (H)	R_s (Ω)	R_{SEI} (Ω)	C_{SEI} (F)	R_{ct} (Ω)	C_{dl} (F)	R_{wo} (Ω)	T_{wo} (s)
2.0	Low	1.76E-06	7.33	2.95	7.42E-06	14.95	1.38E-05	29.78	21.28
2.0	High	1.55E-06	8.42	1.91	1.95E-06	1.95	4.99E-05	5.87	4.89
4.0	Low	1.75E-06	7.37	2.68	5.39E-06	4.17	6.49E-04	9.90	9.87
4.0	High	1.45E-06	7.88	1.84	2.79E-06	1.98	5.43E-05	7.16	8.02

Table 3
Measured dc capacitance vs. EIS determined capacitance.

U (V)	SLMP loading	$C_{Measured}$ (F)	C_{wo} (F)	Percent difference
2.0	Low	0.70	0.71	1.92%
2.0	High	0.90	0.833	7.72%
4.0	Low	1.20	0.99	18.44%
4.0	High	1.37	1.12	20.03%

dependent on the potential of the anode. However, our previous studies showed that too much SLMP loading would result a low anode potential which promoted solid electrolyte layer growth, thereby, reducing the cycle life of the LIC. The suggested loading of SLMP is 10.3–12.7% of HC at anode.

Acknowledgment

This study is supported by DOE BATT Program through PNNL with contract No. 212964.

References

- [1] J.P. Zheng, J. Electrochem. Soc. 150 (2003) A484.
- [2] J.P. Zheng, J. Electrochem. Soc. 152 (2005) A1864.
- [3] J.P. Zheng, J. Electrochem. Soc. 156 (2009) A500.
- [4] G.G. Amatucci, F. Badway, A. DuPasquier, T. Zheng, J. Electrochem. Soc. 148 (2001) A930.
- [5] G.G. Amatucci, F. Badway, J. Shelburne, A. Gozdz, I. Plitz, A. DuPasquier, S.G. Menocal, in: Proceedings of the 11th International Seminar on Double Layer Capacitors, Florida Educational Seminars Inc, 2001.
- [6] S. Tasaki, N. Ando, M. Nagai, A. Shirakami, N. Matsui, and Y. Hato, US Patent Number 7,733,629 B2, 2010.
- [7] H. Konno, T. Kasashima, K. Azumi, J. Power Sources 191 (2009) 623.
- [8] M. Schroeder, M. Winter, S. Passerini, A. Balducci, J. Electrochem. Soc. 159 (2012) A1240.
- [9] N. Böckenfeld, R. Kühnel, S. Passerini, M. Winter, A. Balducci, J. Power Sources 196 (2011) 4136.
- [10] A. Krause, P. Kossyrev, M. Oljaca, S. Passerini, M. Winter, A. Balducci, J. Power Sources 196 (2011) 8836.
- [11] T. Aida, I. Murayama, K. Yamada, M. Morita, Electrochem. Solid-State Lett. 10 (2007) A93.
- [12] T. Aida, I. Murayama, K. Yamada, M. Morita, J. Electrochem. Soc. 154 (2007) A798.
- [13] H. Wang, M. Yoshio, J. Power Sources 195 (2010) 389.
- [14] J. Kim, J. Kim, Y. Lim, J. Lee, Y. Kim, J. Power Sources 196 (2011) 10490.
- [15] S.R. Sivakkumar, A.S. Milev, A.G. Pandolfo, Electrochim. Acta 56 (2011) 9700.
- [16] S.R. Sivakkumar, A.G. Pandolfo, Electrochim. Acta 65 (2012) 280.
- [17] A. Brandt, A. Balducci, Electrochim. Acta 108 (2013) 219.
- [18] M. Schroeder, M. Winter, S. Passerini, A. Balducci, J. Power Sources 238 (2013) 388.
- [19] P.H. Smith, T.N. Tran, T.L. Jiang, J. Chung, J. Power Sources 243 (2013) 982.
- [20] F. Xu, C.H. Lee, C.M. Koo, C. Jung, Electrochim. Acta 115 (2014) 234.
- [21] J. Zhang, Z. Shi, C. Wang, Electrochim. Acta 125 (2014) 22.
- [22] D. Puthusseri, V. Aravindan, S. Madhavi, S. Ogale, Electrochim. Acta 130 (2014) 766–770.
- [23] J.J. Ren, L.W. Su, X. Qin, M. Yang, J.P. Wei, Z. Zhou, P.W. Shen, J. Power Sources 264 (2014) 108–113.
- [24] M. Schroeder, S. Menne, J. Segalini, D. Saurel, M. Casas-Cabanas, S. Passerini, M. Winter, A. Balducci, J. Power Sources 266 (2014) 250–258.
- [25] B. T. Dover, C. W. Kamienski, R. C. Morrison, and R. T. Currin, US Patent Number 5567474, 1996.
- [26] Dover, C. W. Kamienski, R. C. Morrison, R. T. Currin, and J. A. Schwindeman, US Patent Number 5776369, 1998.
- [27] Y. Li, B. Fitch, Electrochem. Commun. 13 (2011) 664.
- [28] C.R. Jarvis, M.J. Lain, Y. Gao, M. Yakovleva, J. Power Sources 146 (2005) 331.
- [29] C.R. Jarvis, M.J. Lain, M.V. Yakovleva, Y. Gao, J. Power Sources 162 (2006) 800.
- [30] M.W. Forney, M.J. Ganter, J.W. Staub, R.D. Ridgley, B.J. Landi, Nano Lett. 13 (9) (2013) 4158.
- [31] J.P. Zheng, W.J. Cao, in: The 20th International Seminar on Double Layer Capacitors and Similar Energy Storage Devices, Florida Educational Seminars Inc, 2010.
- [32] W.J. Cao, J.P. Zheng, J. Power Sources 213 (2012) 180.
- [33] W.J. Cao, J.P. Zheng, J. Electrochem. Soc. 160 (2013) A1572.
- [34] W.J. Cao, J. Shih, J.P. Zheng, T. Doung, J. Power Sources 257 (2014) 388–393.
- [35] K.N. Allahar, D. Battocchi, G.P. Bierwagen, D.E. Tallman, J. Electrochem. Soc. 157 (2010) C95.
- [36] H. Blanke, O. Bohlen, S. Buller, R.W. De Doncker, B. Fricke, A. Hammouche, D. Linzen, M. Thele, D.U. Sauer, J. Power Sources 144 (2005) 418–425.
- [37] P. Mauracher, E. Karden, J. Power Sources 67 (1997) 69–84.
- [38] S. Rodrigues, N. Munichandraiah, A.K. Shukla, J. Solid State Electrochem. 3 (1999) 397–405.
- [39] M.D. Levi, J. Electrochem. Soc. 146 (1999) 1279.
- [40] P. Sharma, T.S. Bhatti, Energy Convers. Manag. 51 (2010) 2901–2912.
- [41] M. Greenleaf, H. Li, J.P. Zheng, Sustain. Energy IEEE Trans. On (2013) 1–6.
- [42] D.D. Macdonald, Electrochim. Acta 51 (2006) 1376–1388.
- [43] M.D. Levi, Z. Lu, D. Aurbach, Solid State Ion. 143 (2001) 309–318.
- [44] H. Song, Y. Jung, K. Lee, L.H. Dao, Electrochim. Acta 44 (1999) 3513–3519.
- [45] M. Nagao, C. Pitteloud, T. Kamiyama, T. Otomo, K. Itoh, T. Fukunaga, K. Tatsumi, R. Kanno, J. Electrochem. Soc. 153 (2006) A914–A919.
- [46] W.J. Cao, Y.X. Li, B. Fitch, J. Shih, J.P. Zheng, J. Power Sources 268 (2014) 841–847.
- [47] W.J. Cao, J.S. Zheng, D. Adams, T. Doung, J.P. Zheng, J. Electrochem. Soc. 161 (14) (2014) A2087–A2092.